ACS OMEGA

Open Access

http://pubs.acs.org/journal/acsodf

Article

Investigation of NaCl-Modified Graphitic Carbon Nitride for Efficient Biodiesel Production from Waste Oil via Transesterification: A Box−Behnken Design Approach

Yichao Hu, Peng Jiang, Yueqin Song, Fangyuan Xiang, and Xiaolong Zhou*

Cite This: *ACS Omega* 2024, 9, 15641−15649

Read Online

ACCESS | Metrics & More | Article Recommendations | Supporting Information

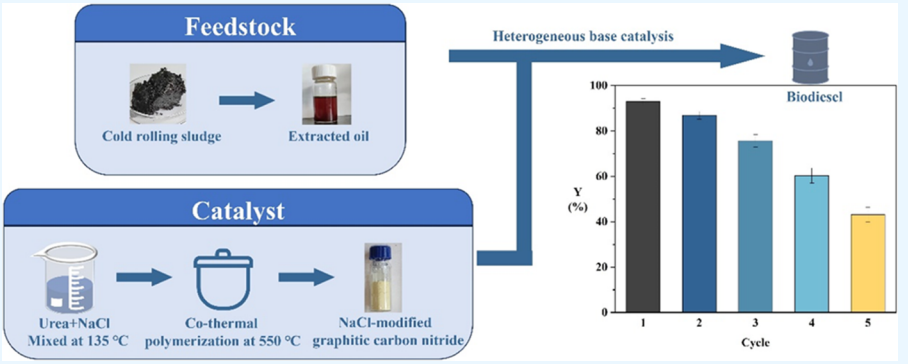

ABSTRACT: NaCl-modified graphitic carbon nitrides (GCN) were applied in the base-catalyzed transesterification of recovered oil. GCN has been seen as a prospective heterogeneous catalyst for transesterification, but pristine-GCN has a narrow range of applications because of its weak basic sites and small surface area. To overcome these defects, NaCl-modified GCN was prepared through the co-thermal polymerization of NaCl with urea. The doping of NaCl generated C≡N and Na−N species, which enhanced the basicity of the catalyst. Meanwhile, with the assistance of NaCl, GCN was decomposed and produced a large number of small pores of hundreds of nanometers, which contributed to the increase in specific surface area. In addition, the effects of transesterification parameters and their interactions on biodiesel yields were investigated by using Box−Behnken design, and the reaction conditions were optimized. A high biodiesel yield of 93.05% was achieved under the optimal conditions.

1. INTRODUCTION

Due to the growing global demand for energy and the depletion of fossil fuel resources, the search for renewable and environmentally friendly alternative energy sources, such as biodiesel, has gained significant attention. Industrially, homogeneous acid or base catalysts have been used for the transesterification during the biodiesel production processes. But the large amounts of wastewater during catalyst separation and washing have prompted the development of heterogeneous catalysts as an alternative.

The traditional production of biodiesel is based on animal and vegetable oils, which account for 80% of the production cost.[1] In recent years, there has been increasing interest in exploring the production of biodiesel from low-grade and low-cost feedstocks, such as nonedible oils,[2−4] waste cooking oils,[5−7] and microalgae,[8−10] because of advantages in terms of sustainability and cost-effectiveness.

Usually, low-cost oils contain amounts of free fatty acids (FFAs) and water, with which the base catalysts undergo saponification reactions, resulting in the loss of active components of the catalysts and separation difficulties. In this regard, solid acid catalysts (SACs) are more tolerant of FFAs[11] and water because they can simultaneously promote esterification of FFAs and transesterification of triglycerides without saponification.[12] But they generally need harsh reaction conditions. With this in mind, researchers have focused on improving the efficiency of SACs. Recently, high biodiesel yield has been reported for many of these catalysts, such as sulfated zirconia,[13,14] MOFs-derived catalysts,[11,15] sulfonic acid-functionalized carbonaceous material,[2,12] etc.

On the other hand, base catalysis has the advantages of fast reaction rate, mild reaction temperature, and low methanol-oil molar ratio.[16] Moreover, the acid value of the feedstock can be reduced by ways such as base neutralization,[17] extraction,[18]

Received: January 17, 2024
Revised: March 4, 2024
Accepted: March 6, 2024
Published: March 20, 2024

https://doi.org/10.1021/acsomega.4c00544
ACS Omega 2024, 9, 15641−15649

and pre-esterification[19] to make it compatible with base catalysts.

Graphitic carbon nitride (GCN) is a novel carbon-based material that can be synthesized by simple thermal polycondensation from abundant precursors, such as urea and melamine. GCN possesses unique properties and shows promising applications in the fields of environmental protection,[20] energy conversion,[21,22] and catalytic synthesis.[23−25] Compared to other heterogeneous catalysts, this carbon-based material is considered a potential alternative catalyst due to its simple and low-cost synthesis route, as well as its environmentally friendly properties. GCN possesses a certain number of basic sites but is not enough to meet the requirement of transesterification. Related studies have mainly focused on improving the catalytic activity of GCN by using different precursors or modification methods. Tayline[26] prepared different morphologies of GCN, which provided useful insights into the mechanistic aspects of GCN-catalyzed transesterification reactions by decorating the catalyst surface with different functional groups obtained through various treatments during synthesis or the use of different precursors. Sung[27] prepared leaching-resistant Na-modified GCN, which could remain active after 10 cycles, by co-thermal polymerization of melamine and NaOH after ball milling. Meghali[28] modified GCN by heat grafting of bran, which improved the activity and reusability in the transesterification process. Zhang[29] synthesized two-dimensional molybdenum-modified GCN for the transesterification of waste cooking soybean oil.

In this study, NaCl-modified GCN catalysts were prepared by co-thermal polymerization of urea and NaCl for the transesterification of oil recovered from cold rolling sludge (CRS), which is a mixture of waste liquid and slag produced in the cold rolling process.[30−32] The N atoms in GCN have lone-paired electrons and therefore act as Lewis base sites. The doping of NaCl generated C≡N and Na−N species which enhanced the basicity of the catalyst.[27] Meanwhile, with the assistance of NaCl, GCN was decomposed and produced a large number of small pores of hundreds of nanometers, which contributed to the increase of specific surface area.[33] The catalysts were characterized by Fourier transform infrared (FT-IR), X-ray diffraction (XRD), X-ray photoelectron spectroscopy (XPS), scanning electron microscopy (SEM), Brunauer−Emmett−Teller (BET), Inductively coupled plasma - optical emission spectrometry (ICP-OES), and CO_2-Temperature-programmed desorption (TPD). Furthermore, the transesterification parameters were optimized by response surface methodology (RSM) using Box−Behnken Design (BBD) to investigate the effects of catalyst loading, methanol-to-oil molar ratio, reaction temperature, and time. By employing multiple regression and correlation analyses, RSM-BBD yields statistically significant results from a limited amount of work.[34]

2. EXPERIMENTAL SECTION

2.1. Materials. Urea (>99%), NaCl (>99.8%), methanol (>99.9%), hexane (>97%), and ethanol (>99.7%) were purchased from Adamas-β (Shanghai, China). CRS was from a lubricating oil company in China.

2.2. Extraction and Pretreatment of Oil. The three-phase composition of the raw CRS is shown in Table 1. The oil in the sludge was obtained by extraction: a certain mass of sludge with an extractant (hexane and ethanol) was placed in a three-neck flask and stirred for 30 min at 50 °C and a stirring speed of 300 rpm. The mixture was centrifuged at 10,000 rpm for 5 min. The liquid phase was dried under a vacuum at 60 °C to remove solvent and water. After that, the oil was mixed with twice the mass of ethanol and sonicated for 5 min to remove FFAs. The mixture was separated into layers after standing for some time. The oil phase (Figure S1) was collected and dried under vacuum at 60 °C to remove residual ethanol. The properties of the oil prepared for transesterification are shown in Table 2.

Table 1. Content of CRS

three-phase content	value
oil (wt %)	49.83
water (wt %)	13.62
solid (wt %)	36.55

Table 2. Fatty Acid Compositions and Physicochemical Properties of Recovered Oil

properties	value
myristic acid (wt %)	1.64
palmitic acid (wt %)	38.63
linoleic acid (wt %)	11.46
oleic acid (wt %)	42.17
stearic acid (wt %)	6.10
moisture content (wt %)	0.2
acid number (mg KOH·g^{-1})	0.5
ash content (wt %)	0.25

2.3. Catalyst Preparation. 40 g portion of urea was heated with a suitable amount of NaCl at 135 °C until it melted, then magnetically stirred at 200 rpm for 1 min, and transferred to a crucible with a lid while still hot. The crucible was heated in a muffle furnace at 550 °C for 4 h (10 °C/min). After heating, the crucible was immediately removed and cooled in a desiccator. The yellowish solid obtained was ground into powder (Figure S2).

The catalyst obtained by this method was named *x*NaCl-GCN, where *x* denotes the mass of NaCl (g) mixed at a weight of 40 g of urea.

For comparison, GCN without any modification was prepared and named Pristine-GCN (PGCN). It was prepared as follows: 40 g of urea was heated to 550 °C in a crucible with a lid at a ramp rate of 10 °C/min and calcined for 4 h. Follow-up treatment is the same as that for modified GCN.

2.4. Catalyst Characterization. The diffraction patterns were determined by using XRD (D8 Advance). Functional groups in GCN were characterized using FT-IR (Nicolet 6700). The bound form of Na in the modified GCN was investigated by using XPS (ESCALAB 250Xi). The decomposition of GCN was analyzed by using TG (Netzsch TG 209 F3 Tarsus). The elemental composition of C and N in GCN was determined using an elemental analyzer (VARIO EL CUBE). The surface area and pore size distribution (pore diameter and pore volume) were examined by a BET (Micromeritics ASAP 2460). The surface morphology was observed by using SEM (Nova NanoSEM450). The basicity of GCN was investigated using CO_2-TPD (Micromeritics AutoChem II 2920). The amount of Na in the catalysts was obtained using ICP-OES (PerkinElmer 8300).

2.5. Catalytic Transesterification Experiments. Transesterification reaction was carried out to evaluate the catalytic activity of the GCN catalysts. A certain mass of catalyst, oil,

https://doi.org/10.1021/acsomega.4c00544
ACS Omega 2024, 9, 15641−15649

and methanol was placed in a round-bottom flask and magnetically stirred (300 rpm). At the end of the reaction, the catalyst was separated by centrifugation (10,000 rpm). After washing several times with a suitable amount of hexane, the catalyst was dried at 110 °C and recovered. The biodiesel layer was separated after the liquid phase mixture was immobilized overnight and dried at 75 °C for 12 h.

Biodiesel yield was calculated using eq 1

$$\text{Yield [\%]} = (\text{Fatty acid methyl ester [}g\text{]})/(\text{oil [}g\text{]}) \quad (1)$$

Fatty acid methyl esters (FAMEs) were quantified by gas chromatography−mass spectrometry (GC-MS, 7890A-5975C) and calibrated using the internal standard method with methyl heptadecanoate as internal standard.[35]

2.6. Experimental Design. The parameters affecting the transesterification reaction, including catalyst loading, methanol-to-oil molar ratio, temperature, and time, were evaluated with biodiesel yield as the response value. The experimental factors and levels are shown in Table 3. Design of the experiment was generated using Design-Expert software. Based on factorial experimental design, four factors with three levels will give 81 (3^4) runs. However, the runs were fixed to 29 by RSM-BBD, including 5 replicates at the central point. The optimum conditions for the reaction were determined by the response surface curve method.

Table 3. RSM-BBD Factors and Levels of the Independent Parameters for the Transesterification Process

			level		
variable	symbol	unit	−1	0	1
catalyst loading	A	wt %	5	10	15
M:O molar ratio	B	mol:mol	6	15	24
reaction temperature	C	°C	60	75	90
reaction time	D	h	2	5.5	9

3. RESULTS AND DISCUSSION

3.1. The Comparative Analysis of Biodiesel Yields of GCN Catalysts. The catalytic activities of catalysts doped with different NaCl contents were compared. The reaction parameters included a catalyst loading of 10%, methanol/oil molar ratio of 12:1, reaction temperature of 70 °C, and reaction time of 9 h. Biodiesel yields using different catalysts are shown in Figure 1. Due to the weak basicity and small surface area, PGCN has almost no catalytic activity.[27] All of the NaCl-modified GCN catalysts had remarkable catalytic effects, and 0.8NaCl-GCN obtained the highest yield of 92.04%.

3.2. Characterization of Catalysts. The FTIR spectra of GCNs with different NaCl doping values are shown in Figure 2. The broad peaks at 3100−3600 cm^{-1} are attributed to the stretching vibrations of the $-NH_2$ and $-OH$ groups. The structure of s-triazine in the GCN is reflected by the C−N bending vibration at 810 (cm^{-1}) and the complex absorption peaks in the range of 1200−1650 (cm^{-1}), which corresponds to the stretching vibrations of C−N and C═N. In contrast to PGCN, NaCl-modified GCNs show a C≡N stretching

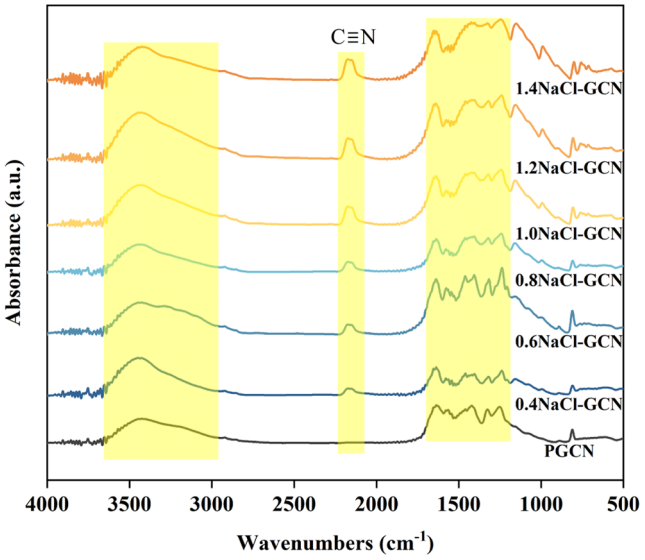

Figure 2. FTIR spectra of the GCN catalysts.

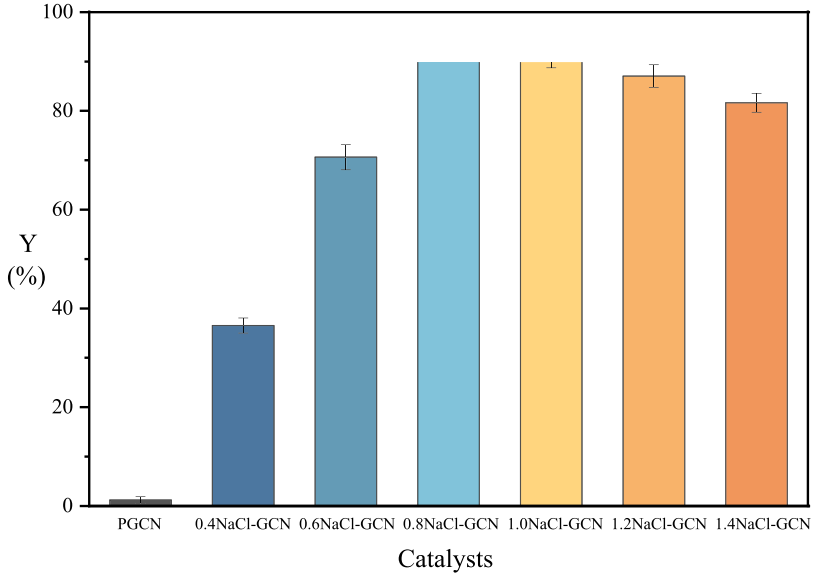

Figure 1. Biodiesel yield over that of GCN catalysts.

https://doi.org/10.1021/acsomega.4c00544
ACS Omega 2024, 9, 15641−15649

vibration peak at 2165 (cm^{-1}).[5] C≡N species act as Lewis base sites and therefore enhance the basicity of the catalyst. Furthermore, the relative intensities of the C≡N absorption peaks increase with the NaCl content.

PGCN and GCNs with different NaCl doping were analyzed by XRD, and the results are shown in Figure 3. PGCN can be

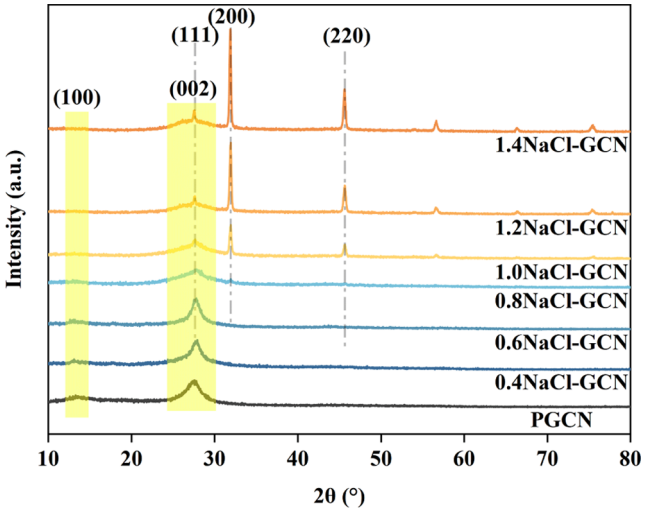

Figure 3. XRD patterns of the catalysts.

recognized by the 27.4° (002) diffraction peak and the 13.1° (100) diffraction peak.[36] With the increase of NaCl doping, the (002) diffraction peak gradually broadened and slightly shifted to a lower angle, reflecting the disruption of the tri-s-triazine structure. After the doping of NaCl was over 1.0 g, several new peaks appeared in the spectrum, including the 27.7° (111) peak, the 31.6° (200) diffraction peak, and the 45.5° (220) peak. These characteristic peaks suggest an excessive NaCl addition, with their intensities further increasing with the amount of NaCl. The excess NaCl may cover the catalyst surface, thereby reducing the exposure of the catalytic sites.

The chemical bonding of Na was further investigated using XPS analysis as shown in Figure 4. The peaks at 1072 and 1071 eV correspond to Na−Cl bond and Na−N bond, respectively.[37] The peak area ratio of Na−Cl and Na−N species in the fresh catalyst before washing treatment is 0.1138, which means that most of the Na atoms exist in the form of Na−N species. Na−N species are considered to have strong basicity and leach resistance.[27] When the catalyst was used and recycled, only the Na−N species were retained.

40 g of urea was melted with 0.8 g of NaCl at 135 °C and mixed with stirring. After cooling, the mixture was ground into powder for TG analysis (30 to 800 °C, at a heating rate of 10 °C/min). As a comparison, TG analysis was also carried out on pure urea after the same treatment as that described above. As shown in Figure 5, the decomposition rate of NaCl-doped urea was faster compared to pure urea. During the polymerization process, NaCl and oxygen in the air will jointly promote the formation of porous structure of GCN.[33]

To further demonstrate the assistance of NaCl in the formation of porous structure, as seen in Table 4, the surface area, pore volume, and average pore diameter of PGCN and 0.8NaCl-GCN were obtained by BET analysis. For PGCN, during the polymerization process, oxygen in urea was converted to H_2O gas.[26] The H_2O bubbles burst, and the ensuing gas pressure leads to structural changes. The surface area and pore volume of GCN increased significantly with the incorporation of NaCl.[38] The adsorption isotherm of 0.8NaCl-GCN is a typical IV isotherm generated by mesoporous solids. As shown in Figure 6, hysteresis loops can be observed. The average pore diameter of the GCN catalysts is about 35 nm, which reduces the diffusion barrier of the reactants and makes it suitable for transesterification.[39]

The surface morphologies of the GCN catalysts were examined by the SEM technique, as shown in Figure 7. The PGCN catalyst exhibits a flake-like structure, while the modified catalyst surface appears as amorphous particles and has a fragmented porous structure, which is caused by the production of gases during the polymerization process. The catalyst particles have a diameter distribution of one hundred to several hundred nanometers. With further doping, the excess NaCl could lead to the agglomeration or inhomogeneous distribution of the active components in the catalyst.

CO_2-TPD analysis was performed on GCN catalysts to determine the strength of the basic sites. As seen in Figure 8, within the temperature range of 50−150 °C, PGCN shows weak basic characteristics, while the peaks of modified GCN catalysts are stronger and shifted toward higher temperatures, which indicates a significant base enhancement. Furthermore,

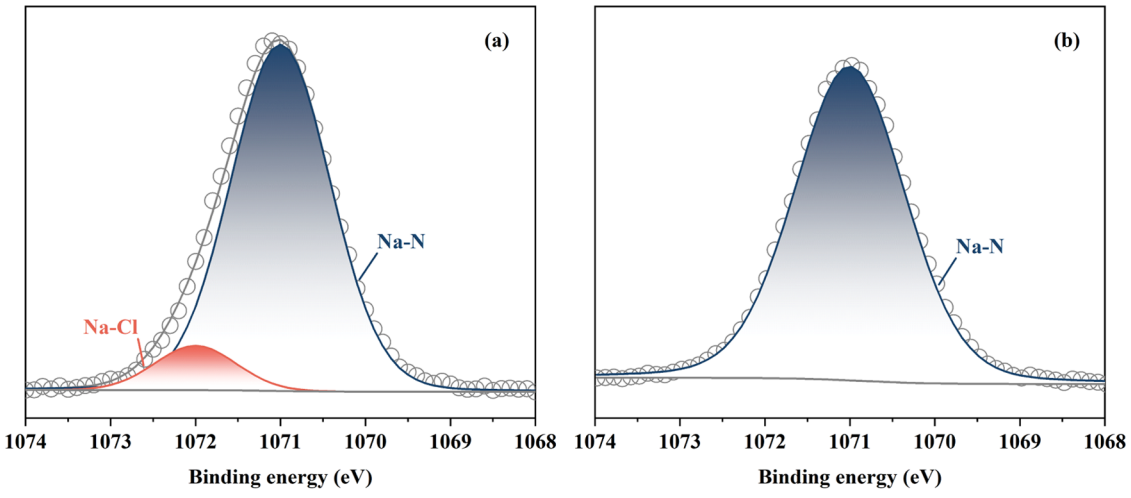

Figure 4. Na 1s XPS spectra of (a) fresh 0.8NaCl-GCN catalyst without washing treatment and (b) recovered 0.8NaCl-GCN catalyst.

https://doi.org/10.1021/acsomega.4c00544
ACS Omega 2024, 9, 15641−15649

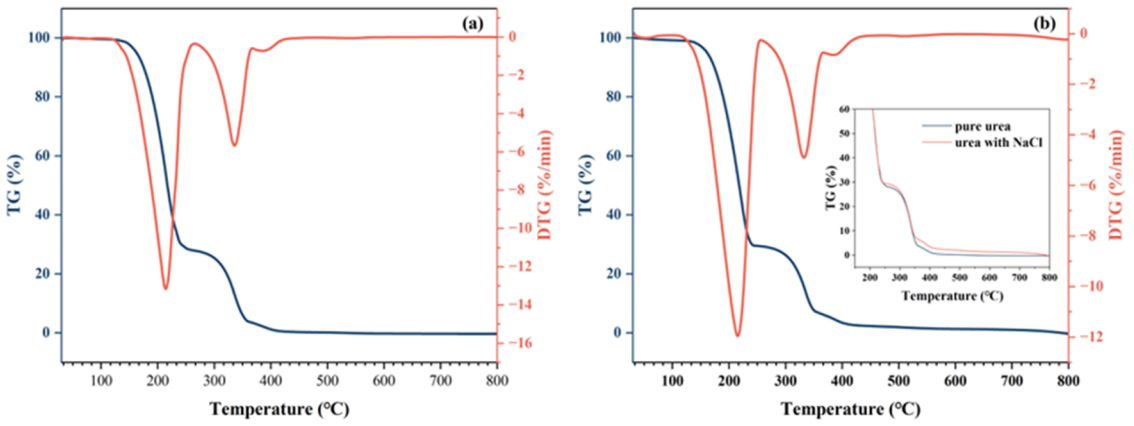

Figure 5. TG-DTG thermograms of (a) pure urea and (b) urea with NaCl.

Table 4. BET Surface Area, Pore Volume, and Average Pore Diameter of GCN Catalysts

catalysts	S_{BET} ($m^2 \cdot g^{-1}$)	pore volume ($cm^3 \cdot g^{-1}$)	average pore diameter (nm)
PGCN	8.76	0.01093	34.57
0.8NaCl-GCN	38.50	0.07259	35.12

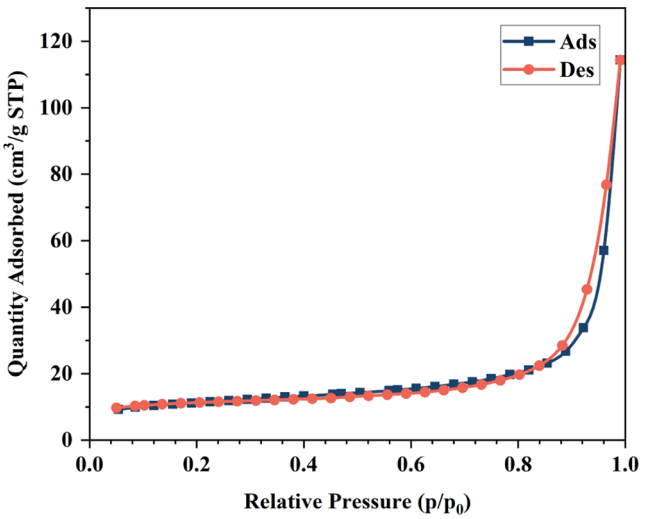

Figure 6. Isotherm linear plot of 0.8NaCl-GCN.

another remarkable desorption peak of modified GCN catalysts appears at about 500 °C, which is related to the strong basic sites of Na−N species. Several weaker desorption peaks appeared between 300 and 400 °C, which might represent primary amines, secondary amines, and weakly basic sites attached to the surface hydroxyl groups.[5]

3.3. Modeling and Parameter Optimization of Transesterification Reaction. *3.2.1. Model Fitting.* RSM-BBD was performed based on 0.8NaCl-GCN, and the results are shown in Table S1. Quadratic multiple regression equation was fitted using Design-Expert software as in eq 2, where *A*, *B*, *C*, and *D* are the coded values of catalyst loading, M:O molar ratio, reaction temperature, and reaction time, respectively. The coefficients of the four factors and their interactions in the equations are positive, which indicates that all four factors have a positive effect on the transesterification reaction. The coefficients of their respective squared terms are negative, which indicates that when these factors reach a certain level, their effect on biodiesel yield tends to saturate. The catalyst loading appears to have a higher coefficient value compared to other factors, indicating its importance in determining oil conversion yield.

$$\begin{aligned}\text{Yield} = {} & 70.39 + 20.11 \times A + 17.02 \times B + 16.23 \times C \\ & + 18.33 \times D + 14.00 \times \text{AB} + 5.40 \times \text{AC} \\ & + 6.54 \times \text{AD} + 10.35 \times \text{BC} + 8.47 \times \text{BD} \\ & + 1.74 \times \text{CD} - 14.66 \times A^2 - 16.52 \times B^2 \\ & - 7.19 \times C^2 - 11.28 \times D^2 \end{aligned} \quad (2)$$

ANOVA for the Response Surface Quadratic model is shown in Table S2. The *F* value of the model is 20274.97, and the *p*-value is less than 0.0001, which indicates that the model is statistically significant. The *p*-value for Lack of Fit was 0.9710, indicating that there is no significant systematic error in the model. Based on the *p*-value of each parameter, it can be seen that all of the parameters except CD are significant for the response. For RSM-BBD, the *R*-squared value is 0.9984 and Adj *R*-squared value is 0.9967 which shows that the model matches the data well. As shown in Figure 9, the color of the dots represents the value of the response (biodiesel yield). The predicted value of the model is very close to the actual value.

3.2.2. Effects of Interactions. Figure S3 shows the variation of the biodiesel yield under different interactions. This series of pictures are plotted when the other two variables are on the 0 level.

Increasing the catalyst loading leads to an increase in the number of reaction sites. However, an excessive amount of catalyst may result in an increase in the viscosity of the reaction system, preventing the mixing and colliding of methanol and oil.[40] The transesterification process theoretically requires an M:O molar ratio of 3:1. But as a reversible reaction, it usually requires an excess of methanol for the reaction to proceed in a positive direction. However, at an excessive M:O molar ratio, the catalyst is diluted, resulting in the yield of the reaction no longer being enhanced.[41] Moreover, the mixture becomes more emulsified when additional methanol is included, making it harder to retrieve the extra methanol. The transesterification is an endothermic reaction, and increasing the temperature favors the reaction, but overheating causes a large amount of methanol to evaporate and not condense back in time, which reduces the amount of methanol left in the system for the residual reaction. In related studies, the temperature close to the boiling point of methanol is generally chosen as the

https://doi.org/10.1021/acsomega.4c00544
ACS Omega 2024, 9, 15641−15649

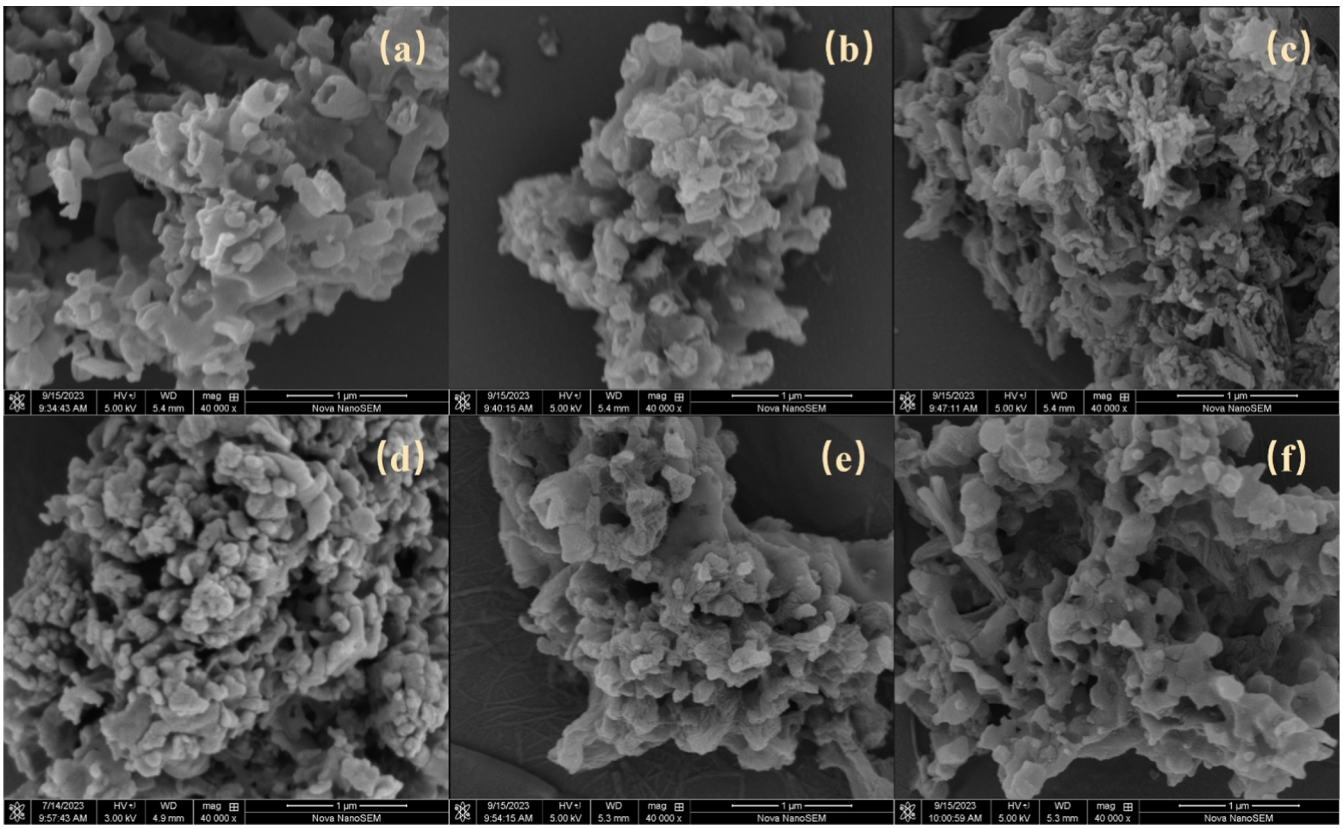

Figure 7. SEM images of (a) PGCN, (b) 0.4NaCl-GCN, (c) 0.6NaCl-GCN, (d) 0.8NaCl-GCN, (e) 1.2NaCl-GCN, and (f) 1.4NaCl-GCN catalyst.

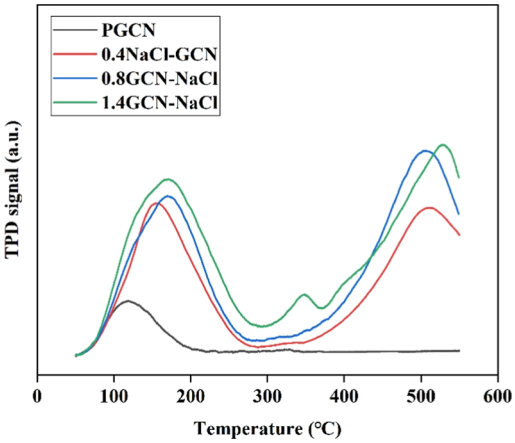

Figure 8. CO_2-TPD profiles of the GCN catalysts.

reaction temperature.[42] For conversion of the reactants to FAMEs as much as possible, an adequate reaction time is necessary. However, an excessively long reaction time may lead to a reversal of the transesterification process.[43]

3.2.3. Optimization and Confirmation of Responses. In the optimization study, the optimization goal for yield was chosen to maximize. In contrast to all other responses, it was chosen to minimize. The optimal parameters were obtained by Design-Expert software, and the validation of the model was carried out under this condition as shown in Table 5. The model recommended the optimal parameters: a catalyst loading of 10.30%, M/O molar ratio of 18.80:1, and reaction time of 6.07 h at 87.1 °C for a predicted yield of 91.90%, which is very close to the actual yield.

3.2.4. Physicochemical Properties of Biodiesel under Optimal Conditions. Some of the physicochemical properties were determined, and the results were in accordance with the ASTM specifications (Table 6). The GC data of the biodiesel obtained from the preparation are shown in Figure S4.

3.2.5. Reusability and Stability of Catalyst. The reusability and stability of the GCN catalyst were further investigated. The recovered catalyst was washed several times with hexane and dried at 110 °C. The 0.8NaCl-GCN catalyst was used 5 times under optimal conditions. As shown in Figure 10, as impurities in the recovered oil gradually contaminated the GCN, the yield of biodiesel decreased from 93.05 to 43.19% in the fifth cycle, while the yield in the fourth cycle remained above 60%. Considering the efficiency and cost, the catalyst can be utilized for at least 4 cycles.

The dissolution of active components into the mixture, especially in polar reaction systems, usually leads to a loss of catalytic activity. In order to show the heterogeneous behavior of the catalytic process, reaction under optimal conditions was paused after 3 h (with a yield of 65.80%) and the GCN catalyst was filtered out of the reaction mixture. Then, the mixture continued to react under the same conditions. A yield of 66.25% was eventually obtained, indicating that the transesterification process was disrupted by the removal of the catalyst.

The 0.8NaCl-GCN catalysts were characterized by ICP-OES to determine the leached Na contents, as shown in Table 7. As mentioned before, most of the Na atoms were transformed into Na−N species. Na−N species are considered to have strong basicity and leach resistance.[27] So, the significant decrease of Na content in the second cycle (14.29 to 12.25%)

https://doi.org/10.1021/acsomega.4c00544
ACS Omega 2024, 9, 15641−15649

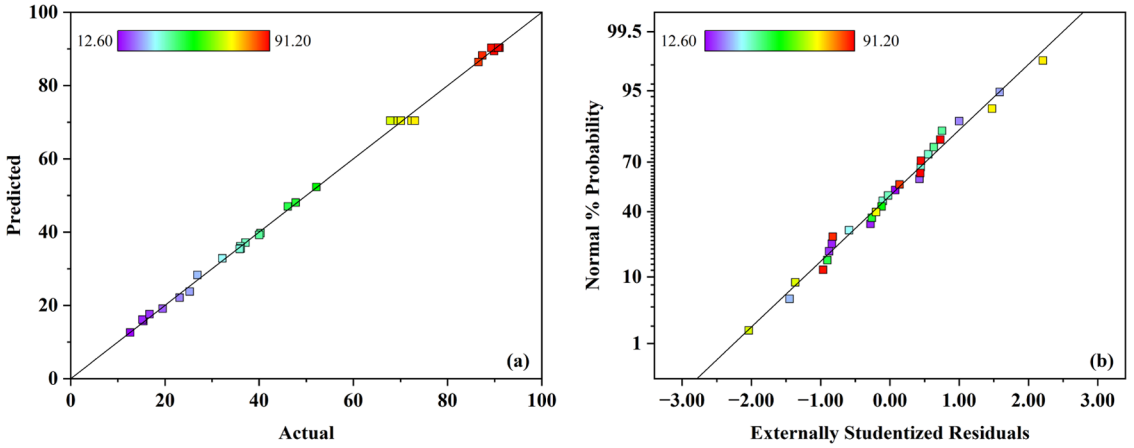

Figure 9. (a) Predicted vs actual and (b) normal plot of residuals.

Table 5. Biodiesel Yield under the Optimized Conditions

catalyst loading (%)	M:O molar ratio (mol:mol)	reaction temperature (°C)	reaction time (h)	predicted yield (%)	actual yield (%)	relative error (%)
10.30	18.80	87.1	6.07	91.90	93.05	1.24

Table 6. Physicochemical Properties of Biodiesel

properties	prepared biodiesel	ASTM D-6751
density (15 °C, g·cm^{-3})	0.88	0.86−0.90
flash point (°C)	167	>130
kinematic viscosity (40 °C, mm^2·s^{-1})	5.2	1.9−6.0
acid number	0.3	<0.50

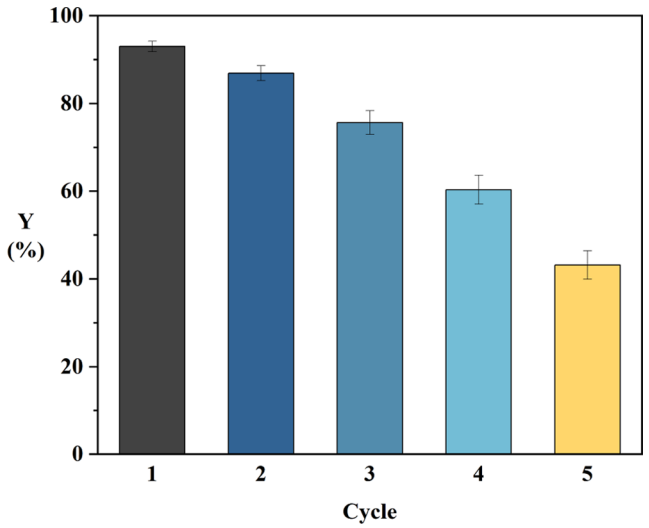

Figure 10. Reusability of 0.8NaCl-GCN.

Table 7. Na Contents of 0.8NaCl-GCN Catalysts

number of cycles	Na contents (wt %)
1	14.29
2	12.25
3	12.12
4	12.07
5	11.84

is attributed to the loss of untransformed NaCl. When the catalyst was used and recycled, only Na−N species were retained. In subsequent cycles, the Na content decreased slightly, suggesting that leaching of the active component may not be the main cause of the loss of catalytic activity.

The deposition of contaminants on the recovered catalyst may account for the loss of catalytic activity. In contrast to conventional feedstocks, the triglycerides in this study were extracted from CRS and therefore contained many impurities, including iron compounds, surfactant, etc. As a waste from the cold rolling process, CRS contains large amounts of iron compounds, some of which exist in the form of fatty acid metal salts[31] (ferric oleate, stearic acid iron, etc.). The extracted oil was characterized by XRD after ashed. As shown in Figure S5, the peptide was identified as Fe_2O_3. The lipophilic iron compounds can hardly be removed from the oil. Typically, surfactants are used in cold rolling emulsion[44] and end up residing in the CRS. The surfactants may form a covering layer on the surface of the catalyst, hindering the contact of reactants with the active sites and leading to a lower yield. Besides, the deposition of organic impurities or intermediate products (such as glycerol and FFAs) on the active sites may also contribute to the decrease in catalytic activity.[45]

4. CONCLUSIONS

Herein, basicity-enhanced GCN catalysts were prepared for catalyzing the transesterification of oil recovered from cold rolling sludge. By simple, highly efficient co-thermal polymerization of NaCl and urea, C≡N and Na−N species with good basicity and leaching resistance were produced in GCN. During the co-thermal polymerization process, NaCl promoted the formation of porous structures, thereby increasing the specific surface area of GCN. The effects of transesterification parameters and their interactions on biodiesel yields were investigated using RSM-BBD. A high yield of 93.05% was achieved using 0.8NaCl-GCN as the catalyst, with a catalyst loading of 10.30%, M/O molar ratio of 18.80, reaction temperature of 87.1 °C, and reaction time of 6.07 h. After four cycles, a more than 60% yield was still available. The main reason for the decreased activity is associated with the deposition of contaminants on the recovered catalyst. Although full activity was not retained, such a high residual activity is valuable for practical applications.

https://doi.org/10.1021/acsomega.4c00544
ACS Omega 2024, 9, 15641−15649

■ ASSOCIATED CONTENT

Supporting Information

The Supporting Information is available free of charge at https://pubs.acs.org/doi/10.1021/acsomega.4c00544.

Additional images and data of raw materials, catalysts, and products, including the details of Box−Behnken design (BBD) experiments (PDF)

■ AUTHOR INFORMATION

Corresponding Author

Xiaolong Zhou − *School of Chemical Engineering, East China University of Science and Technology, 200237 Shanghai, China*; Phone: +86 13701700835; Email: xiaolong@ecust.edu.cn

Authors

Yichao Hu − *School of Chemical Engineering, East China University of Science and Technology, 200237 Shanghai, China*; orcid.org/0009-0009-3617-3898

Peng Jiang − *School of Chemistry and Chemical Engineering, Anqing Normal University, 246011 Anqing, China*; orcid.org/0000-0003-3743-6177

Yueqin Song − *School of Chemical Engineering, East China University of Science and Technology, 200237 Shanghai, China*; orcid.org/0000-0001-8225-2292

Fangyuan Xiang − *School of Chemical Engineering, East China University of Science and Technology, 200237 Shanghai, China*

Complete contact information is available at: https://pubs.acs.org/10.1021/acsomega.4c00544

Notes

The authors declare no competing financial interest.

■ ACKNOWLEDGMENTS

This research was sponsored by the Fundamental Research Funds for the Central Universities.

■ REFERENCES

(1) Zulqarnain; Ayoub, M.; Yusoff, M. H. M.; Nazir, M. H.; Zahid, I.; Ameen, M.; Sher, F.; Floresyona, D.; Budi Nursanto, E. A Comprehensive Review on Oil Extraction and Biodiesel Production Technologies. *Sustainability* **2021**, *13* (2), 788.

(2) Ruatpuia, J. V. L.; Changmai, B.; Pathak, A.; Alghamdi, L. A.; Kress, T.; Halder, G.; Wheatley, A. E. H.; Rokhum, S. L. Green Biodiesel Production from Jatropha Curcas Oil Using a Carbon-Based Solid Acid Catalyst: A Process Optimization Study. *Renewable Energy* **2023**, *206*, 597−608.

(3) Akhtar, R.; Hamza, A.; Razzaq, L.; Hussain, F.; Nawaz, S.; Nawaz, U.; Mukaddas, Z.; Jauhar, T. A.; Silitonga, A. S.; Saleel, C. A. Maximizing Biodiesel Yield of a Non-Edible Chinaberry Seed Oil via Microwave Assisted Transesterification Process Using Response Surface Methodology and Artificial Neural Network Techniques. *Heliyon* **2023**, *9* (11), No. e22031.

(4) Rambabu, K.; Bharath, G.; Hai, A.; Show, P. L.; Banat, F.; Manickam, S. Enhancing Biodiesel Production from Waste Date Seed Oil through Ultrasonic-Assisted Optimization: A Sustainable Approach Using Non-Edible Feedstocks. *Chem. Eng. Process - Process Intensif.* **2023**, *194*, No. 109601.

(5) Ataei, N.; Karbasi, A.; Baghdadi, M. Tailoring the Transesterification Activity of MgO/Oxidized g-C3N4 Nanocatalyst for Conversion of Waste Cooking Oil into Biodiesel. *Fuel* **2023**, *347*, No. 128434.

(6) Hamed, H. H.; Mohammed, A. E.; Habeeb, O. A.; Ali, O. M.; Aljaf, O. H. S.; Abdulqader, M. A. Biodiesel Production from Waste Cooking Oil Using Homogeneous Catalyst. *Egypt. J. Chem.* **2021**, *0* (6), 2827−2832.

(7) Wang, C.; Xie, S.; Zhong, M. Effect of Hydrothermal Pretreatment on Kitchen Waste for Biodiesel Production Using Alkaline Catalyst. *Waste Biomass Valorization* **2017**, *8* (2), 369−377.

(8) Zhao, Q.; Han, F.; You, Z.; Huang, Y.; She, X.; Shi, X.; Han, P. Evaluation of Microalgae Biodiesel for Carbon Neutrality Based on the Waste Treatment by the Autotrophic and Heterotrophic Combination. *Energy* **2024**, *291*, No. 130314.

(9) Song, W.; He, Y.; Huang, R.; Li, J.; Yu, Y.; Xia, P. Life Cycle Assessment of Deep-Eutectic-Solvent-Assisted Hydrothermal Disintegration of Microalgae for Biodiesel and Biogas Co-Production. *Appl. Energy* **2023**, *335*, No. 120758.

(10) Angelaalincy, M.; Nishtha, P.; Ajithkumar, V.; Ashokkumar, B.; Muthu Ganesh Moorthy, I.; Brindhadevi, K.; Thuy Lan Chi, N.; Pugazhendhi, A.; Varalakshmi, P. Phycoremediation of Arsenic and Biodiesel Production Using Green Microalgae Coelastrella Sp. M60 − an Integrated Approach. *Fuel* **2023**, *333*, No. 126427.

(11) Xie, W.; Wan, F. Immobilization of Polyoxometalate-Based Sulfonated Ionic Liquids on UiO-66−2COOH Metal-Organic Frameworks for Biodiesel Production via One-Pot Transesterification-Esterification of Acidic Vegetable Oils. *Chem. Eng. J.* **2019**, *365*, 40−50.

(12) Liu, H.; Chen, J.; Chen, L.; Xu, Y.; Guo, X.; Fang, D. Carbon Nanotube-Based Solid Sulfonic Acids as Catalysts for Production of Fatty Acid Methyl Ester via Transesterification and Esterification. *ACS Sustainable Chem. Eng.* **2016**, *4* (6), 3140−3150.

(13) Zhang, Q.; Xie, W.; Li, J.; Guo, L. Bimetallic Zrx-Aly-KIT-6 Modified with Sulfate as Acidic Catalyst for Biodiesel Production from Low-Grade Acidic Oils. *Renewable Energy* **2023**, *217*, No. 119144.

(14) Sakti La Ore, M.; Wijaya, K.; Trisunaryanti, W.; Saputri, W. D.; Heraldy, E.; Yuwana, N. W.; Hariani, P. L.; Budiman, A.; Sudiono, S. The Synthesis of SO4/ZrO2 and Zr/CaO Catalysts via Hydrothermal Treatment and Their Application for Conversion of Low-Grade Coconut Oil into Biodiesel. *J. Environ. Chem. Eng.* **2020**, *8* (5), No. 104205.

(15) Lu, P.; Li, H.; Li, M.; Chen, J.; Ye, C.; Wang, H.; Qiu, T. Ionic Liquid Grafted NH2-UiO-66 as Heterogeneous Solid Acid Catalyst for Biodiesel Production. *Fuel* **2022**, *324*, No. 124537.

(16) Pan, H.; Xia, Q.; Wang, Y.; Shen, Z.; Huang, H.; Ge, Z.; Li, X.; He, J.; Wang, X.; Li, L.; Wang, Y. Recent Advances in Biodiesel Production Using Functional Carbon Materials as Acid/Base Catalysts. *Fuel Process. Technol.* **2022**, *237*, No. 107421.

(17) Shi, L.; Zheng, L.; Zhao, C.; Huang, J.; Jin, Q.; Wang, X. Effects of Deacidification Methods on High Free Fatty Acid Containing Oils Obtained from Sea Buckthron (Hippophaë Rhamnoides L.) Berry. *Ind. Crops Prod.* **2018**, *124*, 797−805.

(18) Sander, A.; Petračić, A.; Zokić, I.; Vrsaljko, D. Scaling up Extractive Deacidification of Waste Cooking Oil. *J. Environ. Manage.* **2022**, *316*, No. 115222.

(19) Bai, H.; Tian, J.; Talifu, D.; Okitsu, K.; Abulizi, A. Process Optimization of Esterification for Deacidification in Waste Cooking Oil: RSM Approach and for Biodiesel Production Assisted with Ultrasonic and Solvent. *Fuel* **2022**, *318*, No. 123697.

(20) Jing, M.; Zhao, H.; Jian, L.; Pan, C.; Dong, Y.; Zhu, Y. Coral-like B-Doped g-C3N4 with Enhanced Molecular Dipole to Boost Photocatalysis-Self-Fenton Removal of Persistent Organic Pollutants. *J. Hazard. Mater.* **2023**, *449*, No. 131017.

(21) Guo, M.; Chen, M.; Xu, J.; Wang, C.; Wang, L. C, N-Vacancies and Br Dopant Co-Enhanced Photocatalytic H2 Evolution of g-C3N4 from Water and Simulated Seawater Splitting. *Chem. Eng. J.* **2023**, *461*, No. 142046.

(22) Li, H.; Li, X.; Xu, X.; Que, L.; Pan, J.; Zhu, M. The Visible Light Photocatalytic H2 Evolution and Degradation Enhancement of G-C3N4/Er:CdSe/SiO2 Ternary Core-Shell Heterojunction with up-

Conversion Fluorescence Auxiliary. *J. Alloys Compd.* **2023**, *940*, No. 168914.
(23) Ghafuri, H.; Jafari, G.; Rashidizadeh, A.; Manteghi, F. Co2+ Immobilized on Highly Ordered Mesoporous Graphitic Carbon Nitride (Ompg-C3N4/Co2+) as an Efficient and Recyclable Heterogeneous Catalyst for One-Pot Tandem Selective Photo-Oxidation/Knoevenagel Condensation. *Mol. Catal.* **2019**, *475*, No. 110491.
(24) Wei, J.; Shen, W.; Zhao, J.; Zhang, C.; Zhou, Y.; Liu, H. Boron Doped G-C3N4 as an Effective Metal-Free Solid Base Catalyst in Knoevenagel Condensation. *Catal. Today* **2018**, *316*, 199−205.
(25) Wu, F.; Du, J.; Liu, N.; Xu, J.; Xue, B. Potassium-Doped Carbon Nitride Supported on SBA-15 for Enhanced Catalytic Knoevenagel Condensation under Mild Conditions. *Appl. Catal., A* **2022**, *641*, No. 118677.
(26) de Medeiros, T. V.; Macina, A.; Naccache, R. Graphitic Carbon Nitrides: Efficient Heterogeneous Catalysts for Biodiesel Production. *Nano Energy* **2020**, *78*, No. 105306.
(27) Eun Kim, S.; Hu Kim, J.; Keun Kim, D.; Chul Ham, H.; Lee, K.-Y.; Joo Kim, H. Na-Modified Carbon Nitride as a Leach-Resistant and Cost-Effective Solid Base Catalyst for Biodiesel Production. *Fuel* **2023**, *341*, No. 127548.
(28) Devi, M.; Barbhuiya, M. H.; Das, B.; Bhuyan, B.; Dhar, S. S. Modified Mesoporous Graphitic Carbon Nitride: A Novel High-Performance Heterogeneous Base Catalyst for Transesterification Reaction. *Sustainable Energy Fuels* **2020**, *4* (7), 3537−3545.
(29) Zhang, W.; Wang, C.; Luo, B.; He, P.; Li, L.; Wu, G. Biodiesel Production by Transesterification of Waste Cooking Oil in the Presence of Graphitic Carbon Nitride Supported Molybdenum Catalyst. *Fuel* **2023**, *332*, No. 126309.
(30) Zhu, S.; Li, T.; Wu, Y.; Chen, Y.; Su, T.; Ri, K.; Huo, Y. Effective Purification of Cold-Rolling Sludge as Iron Concentrate Powder via a Coupled Hydrothermal and Calcination Route: From Laboratory-Scale to Pilot-Scale. *J. Cleaner Prod.* **2020**, *276*, No. 124274.
(31) Fu, Y.; Que, Z.; Shi, J.; Ai, X.; Zou, W. Thermal Behavior and Gas Products of Cold Rolling Oily Sludge by TG-MS and Py-EGA/MS. *Energy Reports* **2022**, *8*, 763−773.
(32) Qin, L.; Han, J.; He, X.; Zhan, Y.; Yu, F. Recovery of Energy and Iron from Oily Sludge Pyrolysis in a Fluidized Bed Reactor. *J. Environ. Manage.* **2015**, *154*, 177−182.
(33) Chen, Z.; Lu, S.; Wu, Q.; He, F.; Zhao, N.; He, C.; Shi, C. Salt-Assisted Synthesis of 3D Open Porous g-C3N4 Decorated with Cyano Groups for Photocatalytic Hydrogen Evolution. *Nanoscale* **2018**, *10* (6), 3008−3013.
(34) Ao, S.; Gouda, S. P.; Selvaraj, M.; Boddula, R.; Al-Qahtani, N.; Mohan, S.; Rokhum, S. L. Active Sites Engineered Biomass-Carbon as a Catalyst for Biodiesel Production: Process Optimization Using RSM and Life Cycle Assessment. *Energy Convers. Manage.* **2024**, *300*, No. 117956.
(35) Cong, W.-J.; Wang, Y.-T.; Li, H.; Fang, Z.; Sun, J.; Liu, H.-T.; Liu, J.-T.; Tang, S.; Xu, L. Direct Production of Biodiesel from Waste Oils with a Strong Solid Base from Alkalized Industrial Clay Ash. *Appl. Energy* **2020**, *264*, No. 114735.
(36) Zhao, Z.; Long, Y.; Luo, S.; Luo, Y.; Chen, M.; Ma, J. Metal-Free C3N4 with Plentiful Nitrogen Vacancy and Increased Specific Surface Area for Electrocatalytic Nitrogen Reduction. *J. Energy Chem.* **2021**, *60*, 546−555.
(37) Zhang, J.; Hu, S.; Wang, Y. A Convenient Method to Prepare a Novel Alkali Metal Sodium Doped Carbon Nitride Photocatalyst with a Tunable Band Structure. *RSC Adv.* **2014**, *4* (108), 62912−62919.
(38) Xue, Y.; Guo, Y.; Liang, Z.; Cui, H.; Tian, J. Porous G-C3N4 with Nitrogen Defects and Cyano Groups for Excellent Photocatalytic Nitrogen Fixation without Co-Catalysts. *J. Colloid Interface Sci.* **2019**, *556*, 206−213.
(39) Du, L.; Li, Z.; Ding, S.; Chen, C.; Qu, S.; Yi, W.; Lu, J.; Ding, J. Synthesis and Characterization of Carbon-Based MgO Catalysts for Biodiesel Production from Castor Oil. *Fuel* **2019**, *258*, No. 116122.
(40) Li, H.; Wang, Y.; Ma, X.; Wu, Z.; Cui, P.; Lu, W.; Liu, F.; Chu, H.; Wang, Y. A Novel Magnetic CaO-Based Catalyst Synthesis and Characterization: Enhancing the Catalytic Activity and Stability of CaO for Biodiesel Production. *Chem. Eng. J.* **2020**, *391*, No. 123549.
(41) Abukhadra, M. R.; Ibrahim, S. M.; Yakout, S. M.; El-Zaidy, M. E.; Abdeltawab, A. A. Synthesis of Na+ Trapped Bentonite/Zeolite-P Composite as a Novel Catalyst for Effective Production of Biodiesel from Palm Oil; Effect of Ultrasonic Irradiation and Mechanism. *Energy Convers. Manage.* **2019**, *196*, 739−750.
(42) Chen, Q.; Wang, A.; Quan, W.; Gong, W. Efficient Synthesis of Biodiesel from Hyoscyamus Niger L. Seed Oil by Base Catalysis. *Fuel Process Technol.* **2023**, *241*, No. 107630.
(43) Narula, V.; Khan, Mohd. F.; Negi, A.; Kalra, S.; Thakur, A.; Jain, S. Low Temperature Optimization of Biodiesel Production from Algal Oil Using CaO and CaO/Al2O3 as Catalyst by the Application of Response Surface Methodology. *Energy* **2017**, *140*, 879−884.
(44) Wu, Y.; Sun, T.; He, Z.; Zeng, X.; Ren, T.; de Vries, E.; van der Heide, E. Study on the Relationship between the Tribological Properties and Oxidation Degree of Graphene Derivatives in O/W Emulsion. *Tribiol. Int.* **2021**, *157*, No. 106875.
(45) Mansoorsamaei, Z.; Mowla, D.; Esmaeilzadeh, F.; Dashtian, K. Sustainable Biodiesel Production from Waste Cooking Oil Using Banana Peel Biochar-Fe2O3/Fe2K6O5Magnetic Catalyst. *Fuel* **2024**, *357*, No. 129821.

https://doi.org/10.1021/acsomega.4c00544
ACS Omega 2024, 9, 15641−15649